Ly49h-Deficient C57BL/6 Mice: A New Mouse Cytomegalovirus-Susceptible Model Remains Resistant to Unrelated Pathogens Controlled by the NK Gene Complex[1]

Nassima Fodil-Cornu,*† Seung-Hwan Lee,‡ Simon Belanger,§ Andrew P. Makrigiannis,§ Christine A. Biron,‡ R. Mark Buller,¶ and Silvia M. Vidal[2]*†

***Cmv1* was the first mouse cytomegalovirus (MCMV) resistance locus identified in C57BL/6 mice. It encodes Ly49H, a NK cell-activating receptor that specifically recognizes the m157 viral protein at the surface of MCMV-infected cells. To dissect the effect of the *Ly49h* gene in host-pathogen interactions, we generated C57BL/6 mice lacking the *Ly49h* region. We found that 36 h after MCMV infection, the lack of *Ly49h* resulted in high viral replication in the spleen and dramatically enhanced proinflammatory cytokine production in the serum and spleen. At later points in time, we observed that MCMV induced a drastic loss in $CD8^+$ T cells in B6.*Ly49h*$^{-/-}$ mice, probably reflecting severe histological changes in the spleen. Overall, our results indicate that $Ly49H^+$ NK cells contain a systemic production of cytokines that may contribute to the MCMV-induced pathology and play a central role in maintaining normal spleen cell microarchitecture. Finally, we tested the ability of B6.*Ly49h*$^{-/-}$ mice to control replication of *Leishmania major* and ectromelia virus. Resistance to these pathogens has been previously mapped within the NK gene complex. We found that the lack of $Ly49H^+$ NK cells is not associated with an altered resistance to *L. major*. In contrast, absence of $Ly49H^+$ NK cells seems to afford additional protection against ectromelia infection in C57BL/6 mice, suggesting that Ly49H may recognize ectromelia-infected cells with detrimental effects. Taken together, these results confirm the pivotal role of the Ly49H receptor during MCMV infection and open the way for further investigations in host-pathogen interactions. *The Journal of Immunology,* 2008, 181: 6394–6405.**

Human cytomegalovirus is an opportunistic pathogen that occurs within human populations (1). As human CMV and mouse CMV (MCMV)[3] bear a homologous gene structure and induce similar pathologies (2), experimental mouse infection provides an excellent model for the study of mechanisms of host response against the virus. Studies using inbred strains of mice have revealed that both innate and acquired immunity are required to counteract MCMV infection. The innate response includes NK cells that control viral replication by both NK cell-mediated cytotoxicity and the production of effector cytokines (3, 4). Several reports demonstrate the importance of efficient NK cell activity against CMV in both human and murine models (5, 6). In mice, susceptibility to MCMV infection is increased when NK cells are depleted within the first few days of infection (7, 8). However, when the depletion of NK cells occurs a few days later, the outcome of the infection is not affected (8). In addition, cytokines produced by dendritic cells (DC) such as IL-12 and type I IFNs modulate NK cell activation and the subsequent innate responses that are mediated by NK cells (9).

Notably, inbred mouse strains vary considerably in their degree of susceptibility to infection with MCMV, as measured by viral load in target organs and overall survival, allowing a genetic approach to map susceptibility or resistance traits (10). A major determinant of host resistance, whose protective effect is mediated by NK cells, maps to the NK gene complex (NKC) encoding the Ly49 family of NK cell receptors (11). MCMV resistance is achieved through Ly49H, an activating NK cell receptor present in resistant C57BL/6 (B6) mice but absent in susceptible strains such as BALB/c (12, 13). The pivotal role of the Ly49H receptor was first demonstrated by the enhancement of MCMV titers after in vivo depletion of $Ly49H^+$ NK cells (12, 14). In addition, *Ly49h* transgenesis and the introduction of the B6 NKC region to a naturally susceptible background of mice was shown to confer resistance to MCMV (15, 16). Moreover, inactivation of the ITAM-containing DAP12 adaptor protein, which transduces activating signals emanating from Ly49H, reverted the resistant MCMV phenotype in B6 mice (17). Ly49H is activated following recognition of m157, a MHC class I-like protein that is encoded by MCMV and expressed at the surface of the infected cell (18, 19). The triggering of the Ly49H receptor by m157 or MCMV-infected cells induces target cell killing in addition to the secretion of several cytokines, followed by a late phase of specific expansion of $Ly49H^+$ NK (19–21). Conversely, infection of B6 mice by a m157-deleted MCMV virus leads to an evasion of NK cell control, indicating that m157 is the only MCMV-encoded ligand recognized by the Ly49H receptor (22).

*Department of Human Genetics and †McGill Centre for the Study of Host Resistance, McGill University, Montreal, Quebec, Canada; ‡Department of Molecular Microbiology and Immunology, Brown University, Providence, RI 02912; §Laboratory of Molecular Immunology, Institut de Recherches Cliniques de Montréal, Université de Montréal, Montréal, Quebec, Canada; and ¶Department of Molecular Microbiology and Immunology, Saint Louis University Medical School, St. Louis, MO 63104

Received for publication November 27, 2007. Accepted for publication August 28, 2008.

The costs of publication of this article were defrayed in part by the payment of page charges. This article must therefore be hereby marked *advertisement* in accordance with 18 U.S.C. Section 1734 solely to indicate this fact.

[1] This work was supported by Canadian Institutes of Health Research Grant MOP-7781 (to S.M.V.) and by National Institutes of Health Grant CA41268 (to C.A.B.).

[2] Address correspondence and reprint requests to Dr. Silvia M. Vidal, Department of Human Genetics, McGill Duff Medical Building, 3775 University Street, Montreal, H3A 2B4 QC Canada. E-mail address: silvia.vidal@mcgill.ca

[3] Abbreviations used in this paper: MCMV, mouse CMV; NKC, NK gene complex; ECTV, ectromelia virus; DC, dendritic cell; pDC, plasmacytoid DC; p.i., postinfection; MHC-II, MHC class II.

Table I. *Primers used in the fine mapping of the 26.6-kb deletion and their predicted amplicon size*

Marker	Primer Sequence		Amplicon Size (bp)
	Forward	Reverse	
D6Ott166	AATAAACTTAAAAGAGTGCTAACA	GGATATCTGGGCTCCTCAAAT	170
D6Ott168	TTAGCAGAGATAAGTATGCAAGGA	TTTTCTAAGTGTGTAGGTGTGTGG	195
D6Ott169	CAACATATAAAGAAACAGGACTTG	AAGTGGTCTCAGTGTCTCAGTGT	318
D6Ott170	GAACTCCTCATAAAACCAGACACT	ACTTGAGAATTCTTTGTTAACCAA	350
D6Ott172	GGAGACTGAAGTGGAGACCTCCTC	CCAACCGATTCCCTGAGAGTTGTC	349
D6Ott174	TTTCCTATCCCACATTTCTCTTTA	CATAGGGGAATGCTCTGATAGTG	104
D6Ott175	ATGCTCTCCCAATAAAGTTGTTA	TGTACAAGAGATCAGGAAATTGAG	289

The *Ly49h* gene stands as an attractive candidate for several susceptibility loci against virus infection previously mapped to the NKC (23), but many of these connections remain to be solidified. These include susceptibility to infection with HSV1 (24), ectromelia virus (ECTV) (25), and with the parasites *Plasmodium berghei* (26) and *Leishmania major* (27). The evidence for NKC involvement, however, is stronger in some cases than in others. For example, using intra-NKC-congenic mice. Pereira et al. (24) mapped HSV1-susceptibility proximal to the *Ly49* cluster, while Hansen et al. (28) showed that susceptibility to *P. berghei* is associated with the NKC-B6 allele and mediated by CD1d-restricted NKT cells, suggesting that *Ly49h* is unrelated to these phenotypes. In contrast, the B6 mouse presents the active, "resistant" allele in ECTV or *L. major* infection. Moreover, mice lacking NK cells or depleted of NK cells become susceptible to these infections (25, 29, 30), suggesting that Ly49H$^+$ NK cells may play a role in the ECTV and *L. major* models.

Thus far, the models currently used in the study of MCMV pathogenesis compare inbred or congenic strains of mice. However, the effect of genetic variations between these strains could influence the immunological response phenotype. Taking advantage of the particular BXD-8 recombinant strain that carries a small deletion spanning the *Ly49h* gene (13), we used a marker-assisted strategy to generate a congenic B6 mouse in which *Ly49h* was deleted. Thus, by comparing C57BL/6 mice and the *Ly49h*-deficient B6.BXD8TyJ-*Ly49h*$^{-/-}$ (hereafter, B6.*Ly49h*$^{-/-}$) mice, we could assess changes solely associated with the presence or the absence of *Ly49h* in pathogen-host interactions. Our results demonstrate that the expression and function of surrounding *Ly49* genes remains normal in these mice despite the absence of the *Ly49h* gene. Nevertheless, infection of B6.*Ly49h*$^{-/-}$ mice with MCMV showed uncontrolled viral growth in the spleen in the early phase of infection. In addition, antiviral cytokines such IFN-α/β, IFN-γ, and IL-12 levels were dramatically increased in the absence of *Ly49h*. A FACS analysis of the spleen cells showed that MCMV induces a massive cell loss that specifically targets the CD8 T cell fraction. Our results suggest that the amplification of the Th1 response observed after the quantification of the IgG1-specific MCMV Abs in the B6.*Ly49h*$^{-/-}$ mice may be the consequence of the early systemic production of Th1 proinflammatory cytokines.

Lastly, we explored possible *Ly49h* requirements during *Leishmania* and ECTV infections. B6.*Ly49h*$^{-/-}$ mice showed unaltered *L. major* footpad lesions compared with B6 controls, excluding *Ly49h* as a candidate gene for *L. major* resistance. In contrast, B6.*Ly49h*$^{-/-}$ mice presented decreased ECTV load in the spleen compared with B6 controls. This result suggested that *Ly49h* behaves as a susceptibility gene and that Ly49H-mediated recognition of ECTV-infected cells has detrimental effects. Overall, B6.*Ly49h*$^{-/-}$ mice appear to be an ideal tool for the dissection of the immune aspects of host-pathogen interactions.

Materials and Methods

Generation of B6.Ly49h$^{-/-}$ mice

C57BL/6 (B6) and BXD8 mice were purchased from The Jackson Laboratory and housed in a pathogen-free animal facility at McGill University. Experimental protocols were developed in accordance with the institutional guidelines of the Canadian Council on Animal Care. A marker-assisted strategy was used to generate C57BL/6 mice carrying the *Ly49h*-deleted segment within the NKC from BXD-8 donor mice (12, 13). Briefly, (BXD-8 $\times$ B6)F$_1$ mice were backcrossed to C57BL/6. Offspring from the N1 generation were genotyped for the donor's deleted segment using *D6Ott175R* and *D6Ott168F* primers (Table I) and were then selected using a total of 52 microsatellite markers across the genome (available upon request).

After six generations of backcrosses and selections, B6.*Ly49h*$^{+/-}$ mice were intercrossed to produce homozygous B6.Ly49h$^{-/-}$ mice. Two rounds of PCR were used to genotype the B6.*Ly49h*$^{+/+}$, B6.*Ly49h*$^{-/-}$, and B6.*Ly49h*$^{+/-}$ offspring. The first PCR used *D6Ott168F* and *D6Ott175R* primers to characterize the 1020-bp product corresponding to the 26.6-kb deletion of the *Ly49h* region (Table I). The second PCR used the *D6Ott151* marker to distinguish *Ly49h* heterozygous from homozygous mice. A genome scan using 543 single nucleotide polymorphism discriminating B6 and DBA/2 showed 100% inheritance of B6 alleles in B6.*Ly49h*$^{-/-}$ and B6.*Ly49h*$^{+/+}$ littermates, which were independently bred to produced the mice used in this study.

Mouse infections

A Smith strain viral stock was originally obtained from the American Type Culture Collection (ATCC VR-1399, lot 1698918) and was propagated by two passages in salivary glands of weaning BALB/c mice (31). For the experiments, a minimum of five mice ranging from 7 to 10 wk of age were infected by the i.p. route with 5×10^3 PFU of MCMV in 200 μl of PBS. The livers and spleens were collected at various time points. Viral titer was calculated with plaque-forming assays in BALB/c mouse embryonic fibroblast monolayers as previously described (13, 31).

Leishmania major Friedlin V9 was routinely cultured at 27°C in M199 medium (pH 7.4) as previously described (32). Promastigotes were washed in PBS and counted. Mice (a minimum of six mice per group) were infected s.c. in their hind footpads with 5×10^6 stationary phase promastigotes in 100 μl of PBS/mouse. Disease progression was monitored by taking caliper measurements of swelling in the footpads on a weekly basis.

For ECTV infections, 20 mice of each genotype were inoculated i.v. with 100 μl of plaque-purified ECTV (Moscow strain) at 2.0×10^3 PFU/mouse or in the right footpad with 25 μl of 5×10^1 0 or 5×10^2 PFU of ECTV diluted in PBS (33). To monitor viral load, spleens and livers were removed aseptically from mice and frozen at −70°C. Organs were ground and the lysates were frozen and thawed three times, sonicated, and titrated. Virus infectivity was expressed as $\log_{10}$ PFU per ml of tissue lysate.

Flow cytometry analysis and NK cell-killing assays

Spleens from MCMV-infected mice were removed aseptically at day 3 after infection and gently mashed through a 70-μm nylon mesh screen (BD Biosciences). RBC were lysed with RBC lysis buffer (Sigma-Aldrich) and the remaining cells were resuspended in FACS staining buffer (PBS with 2% FBS and 0.01% sodium azide). The number of live cells was determined by trypan blue exclusion. NK cells were analyzed freshly or after expansion for 3–5 days in RPMI 1640 medium supplemented by 1000 U/ml human IL-2 (NCI Preclinical Repository). To isolate plasmacytoid DC (pDC), spleens were digested by collagenase teased apart by repeating pipetting in $\times$ PBS, 5 mM EDTA, and 5% FCS (PBS/EDTA/FCS) and RBC were lysed using a RBC lysis buffer as previously described (9).

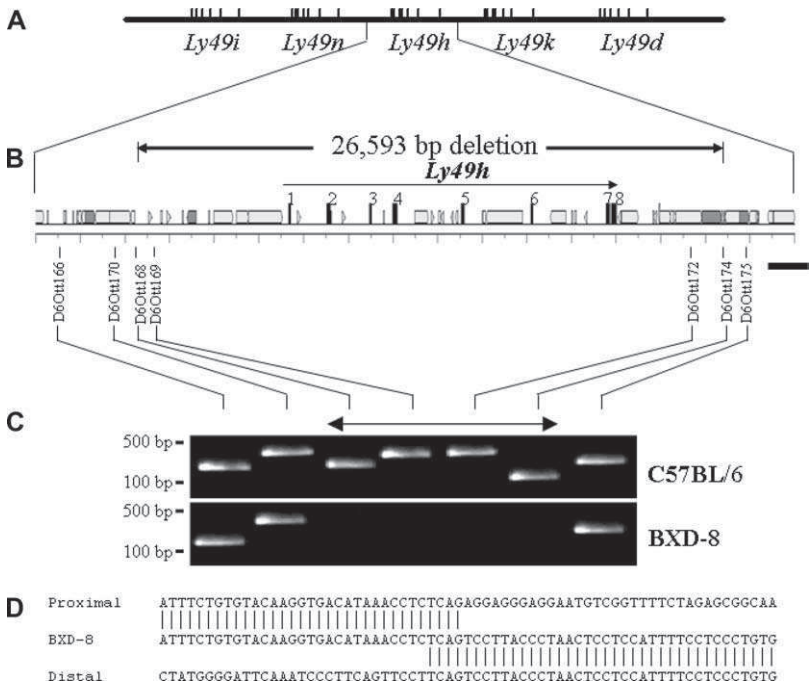

FIGURE 1. Fine mapping of the *Ly49h* deletion in BXD-8 mice. *A*, Physical map in the vicinity of *Ly49h* gene. *B*, Gene structure of *Ly49h* gene. Exons are indicated as black boxes and are numbered 1–8. Gray boxes correspond to repeated sequences. The position of genetic markers used is indicated below. Markers *D6Ott68*, *72*, and *74* are deleted in BXD-8 mice. *C*, STS content analysis of C57BL/6 and BXD-8 DNA with marker across the *Ly49h* genomic domain indicated in *B*. *D*, Sequence of the deleted BXD8 allele at the breakpoint. The proximal and distal sides of the deletion overlap by 4 bp.

Before staining with specific Abs, Fc receptors were blocked by incubating the cells with 5 μg/ml 2.4 G2-blocking Ab for 10 min at 4°C. mAbs directly conjugated to FITC, PE, biotin, and allophycocyanin were used in the immunofluorescence analysis as follows: CD4-FITC, CD8-PE, B220-allophycocyanin, NK1.1-PE, MHC class II (MHC-II)-allophycocyanin, CD69-PE, (eBioscience), CD3-FITC, CD11c-PE, DX5-PE, Ly49D-FITC, Ly49C/I-FITC, LY49G-FITC, Ly49A-FITC, Ly6C-FITC (BD Pharmingen), PE-PDCA1 (Miltenyi Biotec), and *Ly49Q-FITC* (MBL International). The anti-Ly49H-Ab was provided by Dr. W. Yokoyama (Washington University School of Medicine, St. Louis, MO) and was biotinylated using an EZ-Link *N*-hydroxysulfosuccinimide-biotinylation kit (Pierce). Analysis was performed with a FACSCalibur flow cytometer (BD Biosciences) and the data were analyzed with CellQuest (BD Biosciences).

NK cell-killing assays

NK cell activity was determined in NK cell cytotoxicity assays as previously described (34). Briefly, freshly explanted NK cells were washed with PBS, resuspended in complete RPMI 1640 medium, and seeded into wells of a 96-well, round-bottom microtiter plate in graded dilutions to obtain the desired E:T ratios. Target cells (RMA, RMA-S, Chinese hamster ovary (CHO), and YAC-1) were labeled with 100 μCi of $Na_2{}^{51}CrO_4$ (ICN Biomedicals) for 1 h at 37°C, washed three times, resuspended in complete RPMI 1640 medium, and added to the microtiter plate at a concentration of 5×10^3 cells/well. The microtiter plate was then incubated for 4 h at 37°C and 5% CO_2 in a 95% humidified atmosphere. Following centrifugation of the microtiter plate, 100 μl of supernatant was collected from each well, and ^{51}Cr release (in cpm) was ascertained by gamma counting. Percentage of specific lysis was determined by the following equation: percent lysis = $(E - S)/(M - S) \times 100$, in which E is the release from experimental samples, S is the spontaneous release, and M is the maximum release upon lysis with 10% SDS.

Histology

Livers and spleens were isolated, fixed in 10% buffered formalin, and embedded in paraffin. Tissue sections (5 μm) were stained with H&E and analyzed microscopically. Inflammatory foci were defined as discrete clusters of at least 10 individual, small, nucleated cells visible throughout the liver (17, 35, 36). Numbers of inflammatory foci were determined by counting clusters of cells in five randomly selected fields of 1.86 mm^2 each, at a magnification of 100 low-power fields.

Cytokine quantification

Cytokines were quantified from serum and spleen homogenates at day 1.5 postinfection (p.i.) as previously described (37). Briefly, serum was separated from blood cells by 20 min of centrifugation at 4000 rpm and stored at −20°C. Spleen homogenates were prepared in DMEM (2% FBS) and then stored at −80°C. IFN-γ and IL-12 quantification was performed by standard sandwich ELISA according to the manufacturer's (eBioscience) instructions. Type I IFNs were measured using L929 cells in a standard microtiter protection assay against infection with vesicular stomatitis virus as described previously (37).

Anti-IgG1- and IgG2a-specific MCMV detection

Sera isolated on day 0 (uninfected mice) and then on days 15 and 40 were assessed for the presence of anti-IgG1 and IgG2a-specific anti-MCMV Abs by ELISA using an MCMV Ag-coated plate (PL-108; Charles Rivers Laboratories) as described previously (38). Briefly, sera were diluted 60-fold and added to MCMV Ag-coated wells and tissue control wells. Mouse anti-MCMV ELISA control serum (Cl-518; Charles Rivers Laboratories) was used as a positive control. To develop the assay, anti-IgG-1 and IgG-2a HRP (Bethyl Laboratories) was used as recommended by the manufacturer. The net absorbance values (MCMV Ag-tissue control) were converted to score by dividing by 0.13 and multiplying by 10.

Statistical analysis

GraphPad Prism software was used to conduct unpaired, two-tailed Student's t tests for sample analysis. Results with $p < 0.05$ were considered significant.

Results

Characterization of the deleted Ly49h region in BXD-8 mice

Initial mapping studies of the deletion causing the ablation of *Ly49h* localized the proximal limit of the deletion within a 10-kb interval delineated by markers *Ly49k-exon4* and *Ly49h-exon8*, whereas the distal end is localized to a 20-kb interval between *Ly49h-exon1* and *ly49n-exon7* (13). To better delineate the deletion, seven markers, presumably spaced near each end point, were generated using available mouse genomic sequences of the bacteria artificial chromosome clone RP23-128D23 (AC090127, 212,404 bp; Table I). Using the Percent Identity Plot-Marker (PIP-Marker) computer algorithm (http://bio.cse.psu.edu), we analyzed the genomic sequences of the whole *Ly49* gene family and obtained the single locus-specific oligonucleotides. PCR analysis of genomic DNA prepared from B6 and BXD-8 mice indicated that although *D6Ott168*, *D6Ott169*, *D6Ott172*, and *D6Ott174* are located inside the deletion, *D6Ott166*, *D6Ott170*, and *D6Ott175* are located outside its boundaries.

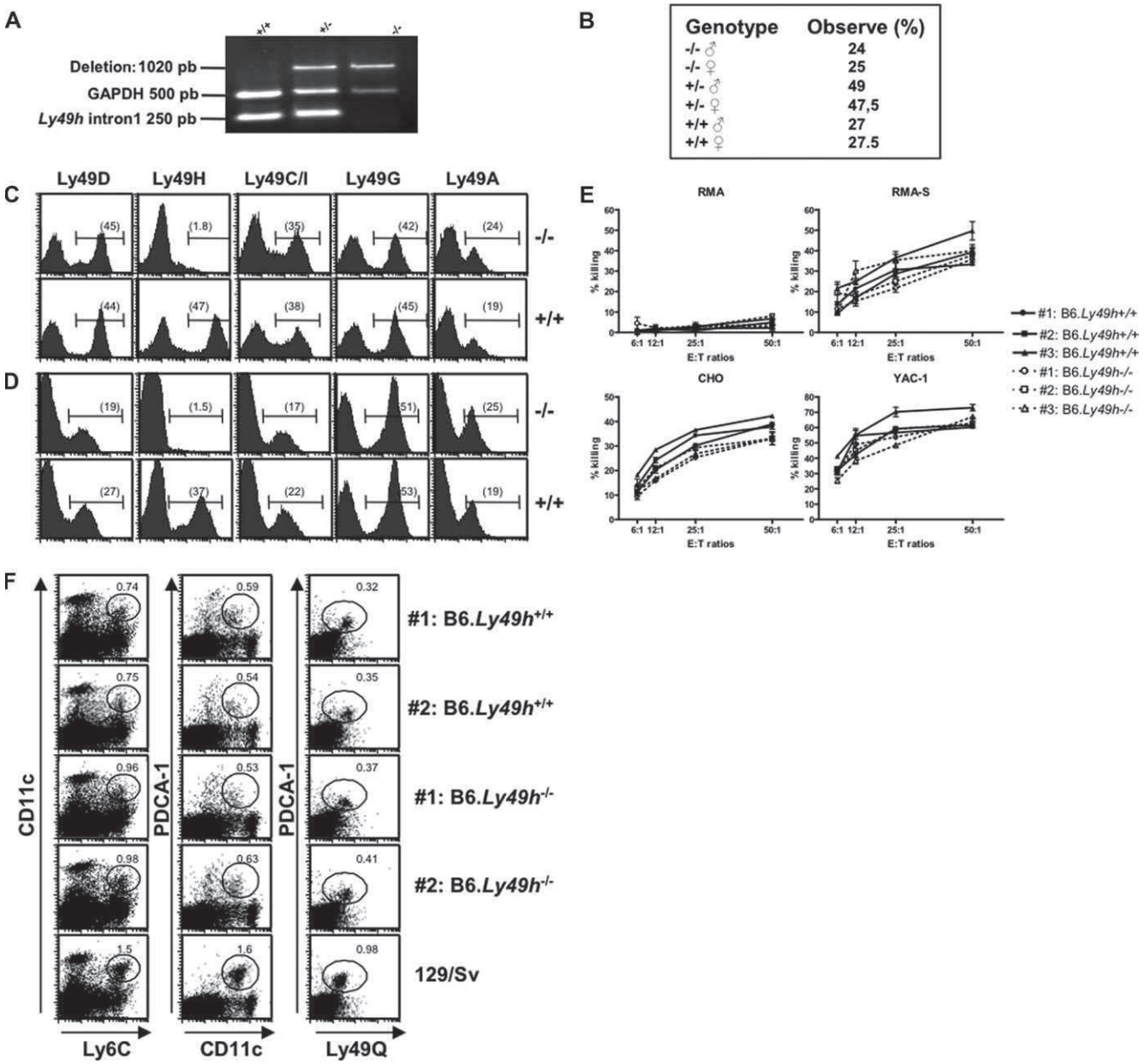

FIGURE 2. Generation, genotyping, and *Ly49* receptors expression analysis of *Ly49h*- deficient mice. *A*, For the genotyping of C57BL/6 $Ly49h^{+/+}$, $Ly49h^{-/-}$, and $Ly49h^{+/-}$ mice, two rounds of PCR were used. The first PCR characterizes the 1020-bp product corresponding to the deletion of the *ly49h* region. *Ly49h* heterozygote and homozygote mice were distinguished by another round of PCR specific for the intron 1 of the *Ly49h* gene using the marker *D6Ott151* (250-bp PCR product). *B*, Classes of offspring observed are as genetically expected. *C* and *D*, *Ly49* genes around the *Ly49h* deletion are normally expressed. Single- cell suspensions of splenocytes (*C*) and IL-2-activated splenocytes (*D*) were prepared and stained with mAb specific for Ly49D, Ly49H (3D10), Ly49C/I, Ly49G, and Ly49A (percentage of positive cells). Cytotoxic activity of lymphokine-activated killer cells from indicated mice was performed against RMA, RMA-S, CHO, and YAC-1 at indicated the E:T ratios (*E*).The frequency of pDC is analyzed by FACS using the indicated Abs (*F*).

PCR analysis using a combination of oligonucleotides flanking the deletion was performed to obtain an amplicon encompassing the deletion breakpoint (Fig. 1). The combination of the forward oligonucleotide of *D6Ott168* (*D6Ott168-F*) and the reverse oligonucleotide of *D6Ott175* (*D6Ott175-R*) amplified an ~1-kb band from the genomic DNA of BXD8 mice but not from B6 mice. This suggested that the 1-kb PCR product spans the deletion breakpoint. Comparison of the complete sequence of the 1-kb amplicon with the B6 genomic sequence of the bacterial artificial chromosome clone RP23-128D23 indicated that the deletion extends over 26,593 bp of genomic DNA and contains the whole genomic region of *Ly49h*. The junction fragment shows perfect alignment with the sequence of both the proximal and distal boundaries without any additional sequence. Moreover, the proximal and distal ends of the deletion overlap by only 4 bp, suggesting that it is unlikely that the deletion is a result of homologous recombination (Fig. 1*D*).

Generation, breeding, and characterization of the B6.Ly49h$^{-/-}$ congenic strain

To facilitate the construction of *Ly49h*-deficient mice with a B6 background, a marker-assisted congenic approach was applied using the pair *D6Ott168-F/D6Ott175-R* and markers located across the DBA/2-originated region of BXD-8 mice (Table I

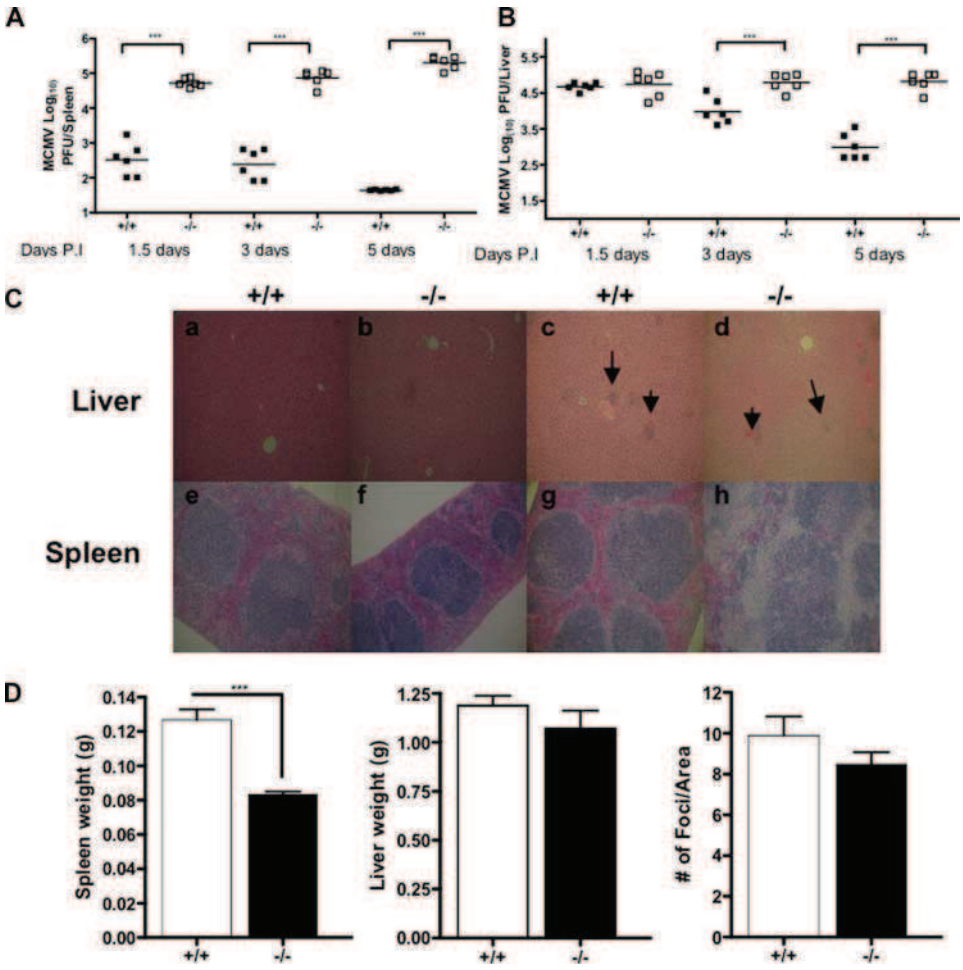

FIGURE 3. B6.*Ly49h*$^{-/-}$ and B6.*Ly49h*$^{+/+}$ mice exhibit different phenotypes upon MCMV infection. *A* and *B*, MCMV titers in the spleen and the liver of B6.*Ly49h*$^{-/-}$ and B6.*Ly49h*$^{+/+}$ mouse strains. Mice were infected with 5000 PFU of MCMV, and the organs were harvested at the indicated times. Viral titer was determined by plaque assays using BALB/c mouse embryonic fibroblast cells. *C*, Histology and evaluation of liver and spleen disease by H&E staining and microscopy analysis of a 5-μm tissue section. *a*, *b*, *e*, and *f* are livers and spleen sections from uninfected mice. *c*, *d*, *g*, and *h* are livers and spleens from infected mice. Inflammatory foci are indicated with an arrow. *D*, Examination of liver and spleen weights on day 3 p.i. The number of inflammatory foci in the liver was determined by counting clusters of cells in three randomly selected fields of 1.86 mm^2 each, at a magnification of $\times$100. Necrotic areas were histologically identified as large, subcapsular, eosinophilic areas of necrotic hepatocytes.

and data not shown). After six generations of marker-assisted selections of progeny with the highest proportion of B6 genomic regions and the *Ly49h*-deleted allele at NKC, a genome scan confirmed that all loci except for the deleted *Ly49h* were reconstituted for B6 homozygosity.

To establish homozygous mice for the *Ly49h* deletion, these mice were intercrossed and their progenies were genotyped using the *D6Ott168-F* and *D6Ott175-R* oligonucleotide pair (flanking the 1020-bp deletion) and the *Ly49h-Intron1* (AF366059) oligonucleotide pair to distinguish between B6.*Ly49h*$^{+/+}$, B6.*Ly49h*$^{+/-}$, and B6.*Ly49h*$^{-/-}$ genotypes (Fig. 2*A*). Mice homozygous for *Ly49h* showed no apparent abnormality and were born at expected ratios (Fig. 2*B*).

To evaluate possible changes in the expression of genes surrounding the 26.6-kb deletion, we determined the surface expression of Ly49 receptors by FACS analysis. As expected, expression of Ly49H was absent on the surface of fresh or activated NK cells from B6.*Ly49h*$^{-/-}$ but not from control littermates. In contrast, the levels of expression of neighboring Ly49 were identical (Fig. 2, *C* and *D*). Moreover, no change was observed in the killing activity of lymphokine-activated killer cells from B6.*Ly49h*$^{-/-}$ and control littermates against a panel of ^{51}Cr-labeled target cells (Fig. 2*E*). In particular, inhibition of killing of RMA cells compared with RMA-S, which lack class I expression, confirmed proper activity of Ly49 inhibitory receptors (39). Cytotoxic activity against CHO cells demonstrated equal function of activating Ly49D (40), while killing of YAC cells showed proper function of NKG2D (41). Taken together, these results suggest that the 26.6-kb deletion affects expression of Ly49H but not expression or function of adjacent genes.

DAP12 null mice have twice the number of pDC than naive control mice and Ly49H signals through DAP12. However, using different Ab mixtures, we found that the frequency of pDC in the spleen of B6.Ly49h$^{-/-}$ mice was equal to control but two times lower than naive 129/Sv mice (Fig. 2*F*). This result indicates that absence of Ly49H does not affect pDC homeostasis.

B6.Ly49h$^{-/-}$ *allow uncontrolled growth of MCMV and show a susceptible histopathological phenotype*

In C57BL/6 mice, we and others have shown that the Ly49H receptor is responsible for controlling MCMV replication in various organs including the spleen and liver (12, 13, 15). To assess the crucial role of the Ly49H receptor, we challenged B6.*Ly49h*$^{-/-}$ mice and littermate controls with 5×10^3, 1×10^4, and 5×10^4 PFU of MCMV. At the highest doses, we found that B6-*Ly49h*$^{-/-}$ mice were significantly more susceptible to MCMV infection than B6 mice, presenting >15% weight loss, piloerection, dehydration, and lethargy as early as 3 days p.i. Upon presentation of these symptoms, mice were humanely sacrificed. In contrast, B6 mice were completely resistant to MCMV-induced disease (data not shown). Moreover, at the lowest dose, viral load in the spleen and liver was analyzed through plaque assay at various time points (Fig. 3, *A* and *B*). The role of Ly49H in the spleen in the early stages of MCMV infection was clearly demonstrated: the viral load in the spleen of B6.*Ly49h*$^{-/-}$ mice at 36 h p.i. was 100-fold higher than in the spleens of the B6.*Ly49h*$^{+/+}$ control mice, with an average PFU count ($\log_{10}$) of 2.0 $\pm$ 0.2 in B6-*Ly49h*$^{+/+}$ and 4.7 $\pm$ 0.0 B6-*Ly49h*$^{-/-}$. This difference increased over the course of infection to reach 4 $\log_{10}$ at day 5 p.i., 1.6 $\pm$ 0.0 B6-*Ly49h*$^{+/+}$

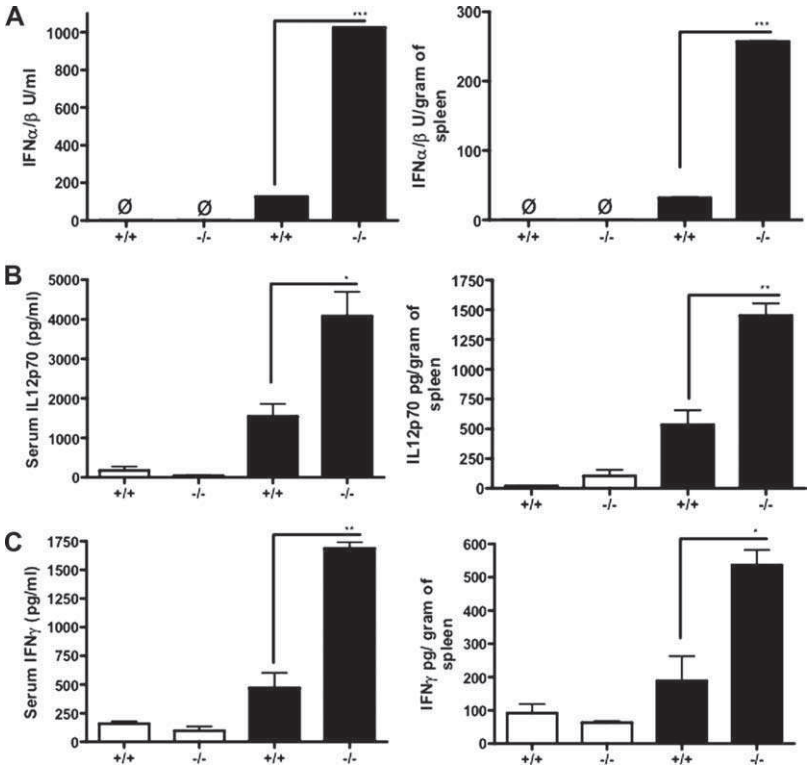

FIGURE 4. Quantification of cytokines in the serum and spleen homogenates on day 1.5 after MCMV infection. Serum or spleen homogenates collected on day 1.5 after MCMV infection as described in *Materials and Methods* were assessed for cytokine levels. *A*, Quantification of IFN-α/β with a bioassay technique using L929 cells. *B*, Quantification of IL-12p70 with ELISA. *C*, Quantification of IFN-γ with ELISA. Black histograms represent infected mice at day 1.5 p.i. White histograms represent noninfected mice. Results are expressed as mean ± SEM of three mice per group. Asterisks indicate statistically significant differences between indicated genotypes (*, $p < 0.05$; **, $p < 0.005$; and ***, $p < 0.001$). ø, Not detected. One of two representative experiments is shown.

and 5.3 ± 0.0 in B6.*Ly49h*$^{-/-}$ mice (Fig. 3*A*). As shown in previous data, in comparison to its effect on the spleen, the role of *Ly49h* in the liver seems to be delayed: by day 3 p.i., there was <1 $\log_{10}$ difference in PFU counts (3.9 ± 0.2 vs 4.7 ± 0.1) which increased to a 2 $\log_{10}$ difference (2.9 ± 0.1 vs 4.8 ± 0.1) by day 5 p.i. between B6.*Ly49h*$^{-/-}$ and B6-*Ly49h*$^{+/+}$ mice (3, 14, 17) (Fig. 3*B*).

To analyze the changes induced by MCMV infection within the liver and spleen, paraffin-embedded sections were stained with H&E (Fig. 3*C*). The control organs from noninfected mice showed healthy architecture, with normal liver parenchymal cells containing granulated cytoplasm, small uniform nuclei arranged around the central vein, and typical red and white pulp regions in the spleen. Consistent with previous reports, in both strains of mice after 3 days of MCMV infection, liver inflammation was distinguished by small inflammatory infiltrates around hepatocytes displaying clusters of nucleated cells (Fig. 3*C*) (7, 14, 17, 42, 43). However, unlike previous studies (14, 44, 45) that reported that mice depleted in NK cells or in subsets of Ly49 receptor-expressing NK cells including Ly49H exhibited a profound pathology in the liver on day 3 p.i., we did not observe any statistically significant difference in terms of weight and number of foci between the livers of B6.*Ly49h*$^{-/-}$ and B6.*Ly49h*$^{+/+}$ mice (Fig. 3*D*). Conversely, in the spleen, significant pathology was observed in B6.*Ly49h*$^{-/-}$ mice, as shown in Fig. 3*C*. The white pulp area in susceptible mice was enlarged and occupied the largest part of the spleen. However, the red pulp area, typically composed of leukocytes and RBC, was considerably diminished in comparison to B6.*Ly49h*$^{+/+}$ or uninfected mice. In addition to these morphological changes in the spleen, a significant reduction in spleen weight was observed in infected B6.*Ly49h*$^{-/-}$ as compared with noninfected mice (data not shown) or B6.*Ly49h*$^{+/+}$ MCMV-infected littermates (Fig. 3*D*). Similar increases in spleen pathology concomitant with a high viral load has been extensively described in numerous models of MCMV infection (10, 14, 44, 46).

B6.Ly49h$^{-/-}$ *mice produce high levels of innate cytokines*

In vivo, the peak production of innate cytokines in immunocompetent strains of mice including 129Sv, BALB/c, and C57BL/6 after MCMV infection occurred at 36 h p.i. We evaluated the impact of the loss of the Ly49H receptor on the early production of cytokines after MCMV infection in vivo. Given the impaired control of MCMV infection in B6.*Ly49h*$^{-/-}$ mice by NK cells, we first analyzed the IFN-α/β production in the serum and the spleen. As shown in Fig. 4, the level of IFN-α/β in infected mice was 10- and 8-fold higher in the serum and the spleen of B6.*Ly49h*$^{-/-}$ mice than in control mice, respectively (Fig. 4*A*). It has been reported that in DAP12-deficient mice the high production of IFN-α/β in response to MCMV infection was due in part to the increased total number of pDC (47). In our experiments, analysis of the pDC proportion using different mixtures of Abs did not reveal an elevated number of splenic pDC in B6.*Ly49h*$^{-/-}$ mice (Fig. 2*F*). In addition to IFN-α/β, IL-12 is also produced by pDC and promotes NK cell activation in part by inducing IFN-γ production (9). To determine the level of IL-12 production as well as NK cell activation, we analyzed the biologically active forms of IL-12, IL-12p70. and IFN-γ in the serum and the spleen of B6.*Ly49h*$^{-/-}$ mice. We found that B6-*Ly49h*$^{+/+}$ mice produced a significantly lower amount of both cytokines in comparison to B6.*Ly49h*$^{-/-}$ mice (Fig. 4, *B* and *C*). The high production of innate cytokines in the absence of the *Ly49h* gene supports the finding that an early control of MCMV replication by NK cells is essential for an efficient and nonsystemic cytokine response.

B6.Ly49h$^{-/-}$ *mice present changes in spleen cell composition during the acute phase of MCMV infection*

We further investigated the composition of spleen cells during the acute phase of MCMV infection. In uninfected mice, *Ly49h*-deficient mice contained a proportion and number of splenocytes comparable to that of the control mice (Fig. 5 and data not shown).

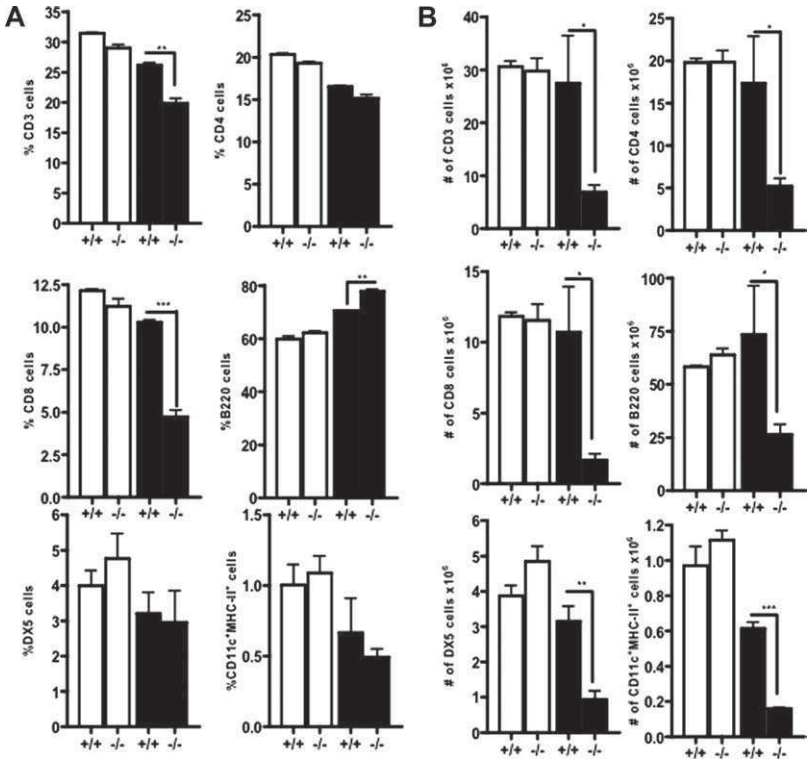

FIGURE 5. Loss of the *Ly49h* gene induces critical changes in the spleen cell component upon infection by MCMV. Splenocytes were harvested from B6.*Ly49h*$^{+/+}$ mice and B6.*Ly49h*$^{-/-}$ mice in uninfected mice (white histograms) or at day 3 post MCMV infection (black histograms) and analyzed for lymphoid populations as described in Material and Methods. (*A*) Represents the percentage of the indicated population. (*B*) Cell enumeration of the indicated population. Results are expressed as Mean ± SEM of three mice per group. Asterisks indicate statistically significant differences between indicated genotypes. (*$p < 0.05$; **$p < 0.005$; ***$p < 0.001$). +/+: B6.*Ly49h*$^{+/+}$ mice; $^{-/-}$: B6.*Ly49h*$^{-/-}$ mice. One experiment representative of at least two is shown.

However, after MCMV infection, especially at day 3, FACS analysis revealed dramatic changes in the proportions (Fig. 5*A*) and numbers (Fig. 5*B*) of spleen cells between B6.*Ly49h*$^{-/-}$ and B6.*Ly49h*$^{+/+}$ mice (no modification in spleen cells was detected at day 1.5 p.i.; data not shown). We observed a significant reduction in the proportion of CD3$^+$ cells in B6.*Ly49h*$^{-/-}$ mice. Interestingly, this reduction did not affect CD4$^+$ T cells but only CD8$^+$ T cells with an average (±SEM) of 10.29 ± 0.14% in B6.*Ly49h*$^{+/+}$ and 4.7 ± 0.41% in B6.*Ly49h*$^{-/-}$ mice. A substantial increase in the B cell proportion was also observed in the B6.*Ly49h*$^{-/-}$ spleen in comparison to B6.*Ly49h*$^{+/+}$ or uninfected mice with an average (±SEM) of 70.48% ± 0.17 in B6.*Ly49h*$^{+/+}$ and 77.79% ± 0.74 in B6.*Ly49h*$^{-/-}$ mice or 62.21% ± 0.69 in B6.*Ly49h*$^{-/-}$ uninfected mice. It must be noted that the B cell proportion was also increased in B6.*Ly49h*$^{+/+}$ in comparison to uninfected mice (Fig. 5*A*).

As previously described, the typical enhancement of MCMV-induced pathology, especially in susceptible mice, was characterized by a drastic loss in total spleen cell number (14, 46, 48, 49). We found at day 3 p.i. an average of 104.4 ± 32.8 million spleen cells in B6.*Ly49h*$^{+/+}$ and 34.35 ± 6.2 B6.*Ly49h*$^{-/-}$. All CD3$^+$ cells, including CD4$^+$, CD8$^+$, cells and B220$^+$, DX5$^+$ cell numbers, were decreased in B6.*Ly49h*$^{-/-}$ mice as compared with B6.*Ly49h*$^{+/+}$ or uninfected mice (Fig. 5*B*). However the most dramatic reduction was observed in the DC compartment (CD11c$^+$MHC-II$^+$). Collectively, our results reveal that the Ly49H receptor plays a critical role in maintaining a homeostatic spleen microenvironment through early control of MCMV infection.

B6.Ly49h$^{-/-}$ *mice have an amplified Th1 response to MCMV*

Pathogens are characterized by their ability to polarize the immune response through Th1 or Th2 responses. MCMV infection induces a strong Th1 response, as evidenced by the production of IFN-γ (42, 50–52). Therefore, we investigated the role of Ly49H in the modulation of the Th response during the chronic phase of MCMV infection by analyzing MCMV-specific B cell responses. We initially analyzed the phenotype of B cells because these cells represented up to 80% of the total cell count after MCMV infection (Fig. 5*A*) and seemed to be preferentially preserved in the spleens of B6.*Ly49h*$^{-/-}$ mice. We found that B cells from B6.*Ly49h*$^{-/-}$ mice present high expression of activation markers CD69 and CD25 (data not shown) compared with B6.*Ly49h*$^{+/+}$ controls (Fig. 6*A*) at day 3 p.i. Subsequently, sera from B6.*Ly49h*$^{+/+}$ and B6.*Ly49h*$^{-/-}$ mice were collected from uninfected and infected mice at days 15 and 40 after MCMV infection to quantify MCMV-specific IgG1 (Th2 response) or IgG2a (Th1 response) levels by ELISA. No difference in terms of IgG1 levels was observed between B6.*Ly49h*$^{-/-}$ and B6.*Ly49h*$^{+/+}$ littermates (Fig. 6*B*). In contrast, at 15 and 40 days p.i., B6.*Ly49h*$^{-/-}$ mice exhibited significantly higher levels of IgG2a in comparison to B6.*Ly49h*$^{+/+}$ mice. Together, these data show that the lack of Ly49H receptors does not radically affect the outcome of the acquired immune response in B6.*Ly49h*$^{-/-}$ mice but may exacerbate the Th1-dependent response to MCMV. Such an increased Th1 response might be linked to the elevated production of IL-12 and IFN-γ observed in B6.*Ly49h*$^{-/-}$ mice at the early phase of MCMV infection.

B6.Ly49h$^{-/-}$ *mice efficiently control* Leishmania *and ectromelia infections*

To further investigate the possible role of *Ly49h* in the control of unrelated NKC pathogen outcomes, we infected B6.*Ly49h*$^{-/-}$ mice with *L. major* and ECTV. The NKC was identified as a candidate region controlling the outcome of cutaneous leishmaniasis using serial backcross mapping of *L. major*-resistance loci from B10.D2 or 129/J-resistant strains onto the susceptible BALB/c background. This revealed that at least 12 loci control the resistance. A significant association between the NKC region in B10.D2 mice (but not 129/J mice) and the trait of *L .major* resistance was identified (27, 53).

Given that mice with a B6 background are closely related to B10 mice and naturally resistant to s.c. infection with *L. major* promastigotes, we assessed the infection of B6.*Ly49h*$^{-/-}$. Footpad

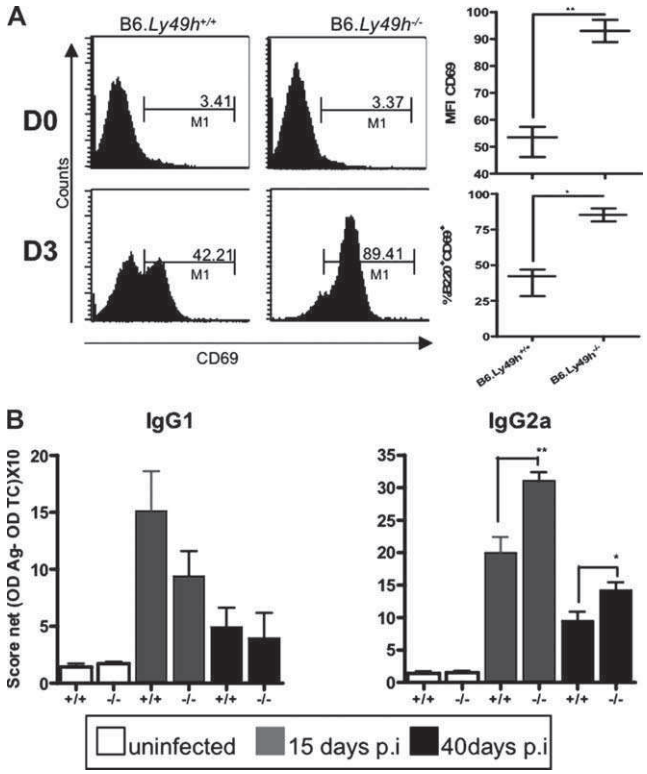

FIGURE 6. Th1 vs Th2 specific Ab response to MCMV in B6.*Ly49h*$^{+/+}$ and B6.*Ly49h*$^{-/-}$ mice. B cells from uninfected (D0) or day 3 (D3) MCMV Infected mice were analyzed with CD69 activating Ab. The MFI or the percentage of CD69 expressing B cells is indicated (*A*). MCMV specific IgG1 (left) and MCMV specific IgG2a (right) were assessed by ELISA in serum from uninfected mice (2 mice per group) or at 15 days and 40 days p.i. with 5000 PFU of MCMV(4–5 mice per group). The net absorbance value (OD MCMV-Ag-OD Tissue Control) X10 was converted to score by dividing by 0.13 (*B*). Asterisks indicate statistically significant differences between indicated genotypes. (*$p < 0.05$; **$p < 0.005$).

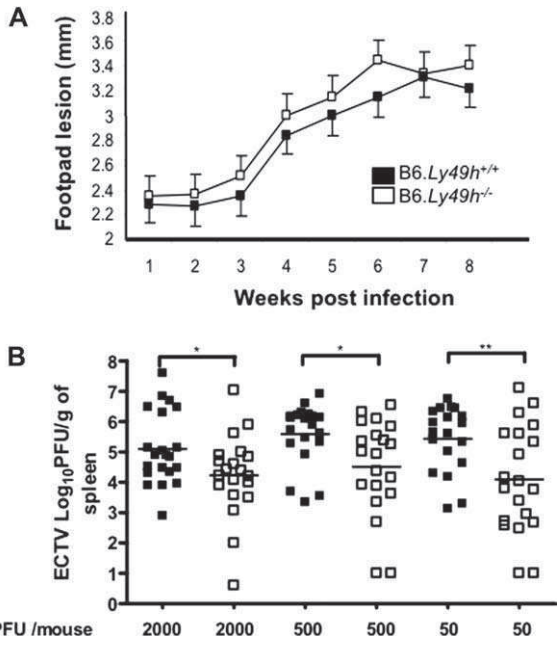

FIGURE 7. *Leismania major* and ECTV infection of B6.*Ly49h*$^{-/-}$ mice. (*A*) Mice were infected with 5×10^6 *Leishmania* promastigotes in their hind footpads. The disease progression was monitored weekly by caliper measurement +/+ : B6.*Ly49h*$^{+/+}$ mice; −/−: B6.*Ly49h*$^{-/-}$ mice. (*B*) Mice were infected through the tail vein with 2000 PFU or their hind footpads with 500 and 50 PFU of ECTV . After 5 days of infection, mice were sacrificed and ECTV titer was assessed in the spleen (*$p < 0.05$; **$p < 0.005$).

necrotic lesions were absent in B6.*Ly49h*$^{-/-}$ and B6.*Ly49h*$^{+/+}$ but observed in susceptible BALB/c control mice (data not shown). However, the kinetics of lesion development after *L. major* infection, as analyzed by weekly scoring of footpad swelling showed a relative but nonsignificant permissiveness to *L. major* infection in B6.*Ly49h*$^{-/-}$ as compared with B6.*Ly49h*$^{+/+}$ mice, with the highest peak occurring at 6 wk (Fig. 7*A*).

ECTV replicates to high titers in the spleen and liver of susceptible mice such as DBA/2 and BALB/c but remains controlled in resistant B6 mice. Mapping studies localized four ECTV-resistance loci (*Rmp1–4*), of which *Rmp1* was mapped to chromosome 6 within the NKC (25).

To analyze the response to severe mousepox, B6.*Ly49h*$^{+/+}$ and B6.*Ly49h*$^{-/-}$ mice were challenged i.v. or in the footpad with three different doses of ECTV (Fig. 7*B*). Mice were sacrificed 5 days later and viral titer was assessed in the spleen and liver. A significant decrease of viral infectivity was observed in the spleens of *Ly49h*$^{-/-}$ mice in comparison with littermates for all infectious doses. The largest difference was observed at a dose of 50 ECTV PFU in the footpad with spleen ECTV loads of $\log_{10}$ 4.0 ± 1.7 PFU in mutant mice and 5.4 ± 1.07 PFU in control mice. No difference was detected in the liver (data not shown).

Altogether, our results showed unaltered resistance to *L. major* in the absence of *Ly49h*. However, in *Ly49h*$^{-/-}$ mice, the ECTV outcome was improved, suggesting a possible detrimental role of the Ly49H receptor in the response to ectromelia.

Discussion

Studies using the BXD-8 mouse strain were instrumental in pinpointing the genetic defect associated with MCMV susceptibility, as the defect harbors a B6 MCMV-resistance haplotype at NKC despite being highly susceptible to MCMV (11). Thereafter, we found that BXD-8 harbored a deletion of the entire encoding region of *Ly49h* between the *Ly49n* and *Ly49k* genes (13). However, BXD-8 is a recombinant inbred strain with a genome composition that is on average 50% of B6 origin and 50% of DBA/2 origin (54). Therefore, several questions relating to the precise role of the Ly49H receptor in physiological conditions or in response to infection could not be solved in this model. In this study, we have taken a two-pronged approach to fill this gap: first, we have further characterized the *Ly49h* deletion present in BXD-8 mice and have used this knowledge to produce *Ly49h*-deficient B6 mice. Second, we have initiated the characterization of the B6-*Ly49h*$^{-/-}$ model in response to various infections under the control of NKC.

DNA sequence analysis of the spontaneous BXD-8 *Ly49h* deletion breakpoint fusion fragments indicates that these junction fragments might be the result of nonhomologous recombination, a mechanism important in the formation of new genes (55). No extensive sequence homologies are observed at the junction of the deletion termini. Moreover, no extraneous nucleotides of unknown origin have been created in contrast to other deletions junctions characterized in mutations of the human β-globin (56) or neurofibromatosis type 1 genes (57). The molecular events by which the *Ly49h* deletion occurred are not clear, although the nature of the deletion junction bears similarity with other deletion mutations in the aforementioned genes (56, 57). DNA sequence analysis of the *Ly49* cluster in B6 mice suggested a region of important genetic fluidity, formed by single and block duplications of genes, deletions, conversions, and other rearrangements resulting in a highly

variable and complex locus in the mouse (58). Moreover, the absence of ancient lineages coupled with the recurrent creation of activating receptors suggests that these receptors are phylogenetically recent (59). Thus, the spontaneous deletion of *Ly49h* in BXD-8 mice may have arisen by the same molecular mechanisms that govern the natural evolution of the *Ly49* family.

Few B6 background models of MCMV infection involving a defect in NK cells have been described. These include defects in granule exocytosis whereby NK cells are incapable of killing infected cells. In *beige* mice, for example, the mutation in the lysosomal trafficking regulator (*Lyst*) gene confers susceptibility to MCMV (6). More recently, the mutation in the *Unc13d* gene provoked a failure in NK and T cell degranulation, inducing an uncontrolled viral spread (60). The distinct role in MCMV infection of perforin (*Prf*) and granzyme (*Gzm*) cytotoxic granules or IFN-γ secretion has been established in *Prf*-, *Gzm*-, and *IFN*-γ-deficient mice (3, 61, 62). Thus far, Ly49H is the only identified activating NK cell receptor that specifically recognizes a MCMV-encoded protein. In this context, the *Ly49h*-deficient mice represent a valuable tool for the study of the impact of a receptor-mediated NK cell response on the control of viral infections.

Our study showed that, in B6 mice, the absence of the *Ly49h* gene does not seem to disturb either the expression or the function of the surrounding genes. However, this absence results in MCMV viral titers in spleen and liver comparable to those of the susceptible BALB/c strain of mice (data not shown). In addition, as previously described, loss of MCMV replication control was accompanied by major changes in the histological structure of the spleen at the time of peak viral growth by 3 days p.i Notably, Benedict and colleagues (46) demonstrated that as a result of MCMV infection spleen microarchitecture is altered through the complete loss of macrophages and loss of B and T cell compartmentalization in the white pulp. Work by Bekiaris et al. (49) indicated that these changes are conspicuous in susceptible BALB/c or NK cell-depleted mice and lead to the destruction of white and red stroma. In contrast, B6 mice or BALB-*Cmv1*^{r} have preserved splenic structure, with NK1.1$^+$ (63), NKp46$^+$ (64), and Ly49H$^+$ cells migrating from the red pulp into the marginal zone, the white pulp and T cell areas. This suggested that Ly49H mediates MCMV resistance through NK cell antiviral activity and by preserving the structure of splenic white pulp (49, 64). These different reports were, however, limited by the specificity of the Abs used or by the very low percentage of cells visualized. In the present report, we used B6-*Ly49h*$^{-/-}$ mice which lack the Ly49H receptor selectively expressed on a subset of NK cells but which possess an intact NK cell compartment. This allowed us to further support previous conclusions by providing unambiguous evidence that the selective loss of the Ly49H receptor results in identical disruption of spleen architecture and uncontrolled virus replication as observed in NK cell-deficient mice.

We observed that B6-*Ly49h*$^{-/-}$ mice have 8–10 times higher liver viral load than controls, providing further evidence of Ly49H-dependent antiviral activity in this organ. However, contrary to the spleen, B6-*Ly49h*$^{-/-}$ and B6-*Ly49h*$^{+/+}$ mice did not present major histological changes in the liver upon MCMV infection. At 3 days p.i., *Ly49h*-deficient mice had identical numbers of mononuclear cell infiltrates and only slightly increased liver pathology (small areas of necrosis) as compared with controls. MCMV-induced liver inflammation is characterized by the accumulation and localization of NK cells in inflammatory foci surrounding infected liver cells (reviewed in Ref. 65). Both NK cells and NK cell-dependent IFN-γ production appear critical to control the number of both the inflammatory and necrotic foci (4). Depletion of NK cell subsets with anti-Ly49H/C/I Ab results in the absence of discrete inflammatory foci and large necrotic areas, which implicated Ly49H$^+$ NK cells in foci formation and control of liver pathology (14). However, DAP12-deficient mice, which express Ly49H but lack Ly49H-mediated signals, show a normal number of foci but present extensive liver necrosis, suggesting that the lack of signaling via Ly49H is not required for foci formation but rather for limiting virus-induced liver disease (17). Our results extend these conclusions, suggesting that lack of Ly49H expression does not appear critical for either foci formation or extensive liver necrosis. Supporting the view that differences in the extent of liver pathology between DAP12-deficient and B6-*Ly49h*$^{-/-}$ mice relate to Ly49H-independent functions of DAP12, there is recent evidence that in DAP12-deficient mice macrophages and DC have an exacerbated cytokine response to MCMV infection (47). This overactive response may participate in the exaggerated liver pathology observed in DAP12 knock-out but not in B6-*Ly49h*$^{-/-}$ mice.

Our results showed that despite bearing 100-fold higher spleen viral load than control mice by 36h p.i., B6.*Ly49h*$^{-/-}$ mice also had dramatically increased IFN-α/β, IL-12, and IFN-γ cytokine levels. At that time, NK cells from B6.*Ly49h*$^{-/-}$ produced two times more intracellular IFN-γ than control mice (data not shown). This is not surprising, given that the production of these three cytokines is intimately intricate. IFN-α/β promotes accumulation of pDC, which likely contributes to the amplification loop of cytokine secretion, including IL-12 (9, 66). Blocking anti-IL-12 Abs abolishes NK cell-dependent IFN-γ production during MCMV infection (4). As mentioned elsewhere, the high production of IL-12 and IFN-α/β in DAP12 null mice in response to MCMV infection was attributed to both a higher proportion of pDC-producing cytokines and an increase in the number of pDC (47). Ly49H/DAP12-dependent signals, however, do not seem to influence homeostasis of pDC since B6.*Ly49h*$^{-/-}$ mice had identical pDC numbers than controls in normal conditions (Fig. 2*F*). Our results are in accordance with those from Robbins et al. (67), which demonstrate that the intensity and duration of IL-12 and IFN-α/β secretion by pDC is decreased in BALB.*Cmv1*^{r} mice (MCMV resistant owing to a B6-congenic fragment at NKC) compared with MCMV-susceptible BALB/c controls. In this case, pDC activity was attributed to the early control of MCMV by NK cells. We confirm and extend these results showing that the specific lack of Ly49H-dependent signals in a B6 background are sufficient to induce uncontrolled systemic cytokine levels.

In B6-*Ly49h*$^{-/-}$ mice, we found that CD8 T cells are lost during MCMV infection. This does not seem to be the consequence of a direct lysis by MCMV infection (68). However, this is consistent with previous results showing that the presence of anti-MCMV-specific CD8$^+$ T cells, which appear at day 4 p.i. in the MCMV-resistant strains of mice, is delayed by high levels of type I IFN (67). In fact, virus-induced lymphopenia has been observed in several acute viral infections such as lymphocytic choriomeningitis virus, influenza, vesicular stomatitis virus (reviewed in Ref. 69), as well as some bacterial infections such as *Listeria monocytogenes* (70, 71). In these studies, it was shown that the common mechanism of CD8$^+$ T cell loss by apoptosis is the consequence of systemic production of type I IFN. These observations suggest that a similar mechanism may be operative in B6-*Ly49h*$^{-/-}$ mice. We also showed that the total number of DCs in the spleen of B6.*Ly49h*$^{-/-}$ mice is dramatically reduced compared with MCMV-infected controls. This probably reflects the loss of CD11b$^+$ and CD8$^+$ DC cells as previously described (67).

During MCMV infection, pDC are the primary producers of type I IFN and also an important source of circulating IL-12 and TNF (9, 47, 66, 72). pDC are not infected by MCMV but are

thought to engulf the debris of infected cells containing viral Ags that simulate TLR7- and TLR9-dependent type 1 IFN secretion (73, 74). Thus, in the absence of viral control by NK cells, continuous uptake of MCMV Ags by these cells may contribute to systemic cytokine production. Dysregulated cytokine production and loss of DC and T cells along with destruction of stromal cells by direct cytopathic MCMV effects (49) may have led to a total disorganization of spleen microarchitecture in B6-*Ly49h*$^{-/-}$ mice, as previously demonstrated in other models (49, 67).

We finally analyzed the role of Ly49H during *L. major* and ECTV infections, which outcomes are under NKC control. Our results indicated that B6-*Ly49h*$^{-/-}$ mice had a slight, although nonsignificant, increase of footpad lesions during the first weeks of infection with *L. major*. Mice infected with *L. major* showed marked genetic differences in disease manifestations: susceptible BALB/c mice exhibit enlarging lesions that progress to systemic disease and death, whereas resistant C57BL/6 mice develop small, self-healing lesions. Although early defense against *L. major* is initiated by both the stimulation of NK cells and the production of IFN-γ (30), our lack of statistical significance is not entirely surprising. Susceptibility to leishmaniasis is influenced by variants at multiple host genes that when considered individually have rather small effects on lesion progression. Such variants collectively, however, may have substantial additive or epistatic effects (75). Consistent with this concept, Beebe et al. (27) found that the NKC locus had a much stronger effect in combination with a locus on chromosome 15 (27), while *H2* has also been found as a susceptibility allele (76). Therefore, to fully asses the role of *Ly49h* in *L. major* infection, it would be important to study its effect in double mutant mice carrying the susceptibility allele on chromosome 15 (from BALB origin) or *H2*^{d}.

Our findings indicated that B6.*Ly49h*$^{-/-}$ mice had 1.5 $\log_{10}$ decreased spleen virus titers than control mice in response to ECTV, suggesting that Ly49H promotes a detrimental effect. These results were unexpected because NK cells are crucial for the early control of ECTV replication via direct antiviral and indirect immune modulator activities (29, 77). Thus NK1.1-depleted B6 mice had 3 $\log_{10}$ and 1.5 $\log_{10}$ higher titers in spleens and livers than controls when infected in identical conditions (50 PFU of ECTV by the footpad route). Moreover, using anti-NKG2D-blocking Abs, Fang et al. (77) showed that NKG2D is an important determinant of B6 resistance to ECTV. In our study, however, NKG2D activity seems intact in *Ly49h*-deficient and control mice as determined by YAC cell killing. NKG2D signals either through DAP10 or DAP12 adapter proteins, but the effect of NKG2D blockage is much more severe than DAP10 or DAP12 deficiency. A possible interpretation of these results is that the adapter proteins have overlapping effects (77). In view of the increased ECTV resistance of B6.*Ly49h*$^{-/-}$ mice, we can postulate that DAP12 deficiency may abolish both protective signals emanating from NKG2D as well as deleterious signals emanating from Ly49H. This would suggest that more than one gene underlies the ECTV-resistance locus *Rmp1*, an event currently found in genetically complex diseases. Similar paradoxical responses have been observed for other innate immune receptors such as TLR3, which mediates either protective or deleterious mechanism depending on the viral infection (78). Furthermore, in some human cancers linked to viruses (e.g., human papilloma virus) and in various autoimmune disorders, the absence of activating NK receptors is associated with a positive outcome of the disease (79–82). Therefore, it is tempting to speculate increased Ly49H-mediated chemokine production in response to ECTV as a possible Ly49H mechanism leading to increased viral load. Poxviruses have the ability to harness cytokine and chemokine production for their own benefit (83). For example, in a model of vaccinia virus infection, deletion of a viral chemokine inhibitor results in increased cytokine levels and viral titer (84). Therefore, it would be interesting to study the role of Ly49H-mediated chemokine production during ECTV infection, its effect on ECTV replication, and the function of the ECTV viral chemokine inhibitor (85) in viral pathogenesis. Our results also suggest Ly49H-mediated recognition of ECTV-infected cells. Using protein homology recognition engines (http://www.sbg.bio.ic.ac.uk/phyre/html/index.html; http://toolkit.tuebingen.mpg.de/hhpred), we identified three ECTV-predicted proteins with structural homology to MHC class I molecules (S. M. Vidal, unpublished data) that may be likely candidates to trigger Ly49H. Analysis of these potential ECTV Ly49H ligands may provide a new line of investigation in ECTV pathogenesis. Recently, using a similar model, it was found that *Ly49*-deficient mice were found to bear a similar level of ECTV quantitative PCR products (86). However, the infectious dose was not indicated and it is not clear whether quantitative PCR products correlate with ectromelia infectious particles, which makes difficult a comparison to the present study. Although this model remains to be fully characterized, *Ly49h*-deficient mice survived challenge by a low and high dose of HSV-1, indicating Ly49H-independent resistance against this pathogen (86).

In summary, the generation and characterization of B6.*Ly49h*$^{-/-}$ mice has allowed us to better define the role of Ly49H-mediated responses during MCMV infection. Moreover, our investigation of ECTV and *L. major* responses demonstrated that this mouse strain is a valuable model to examine the role of Ly49H during infection with unrelated pathogens.

Acknowledgments

We thank Dr. Greg Matlashewski and Dr. Wen-Wei Zhang (McGill University) for the preparation of *Leishmania* promastigotes and Dr. Danielle Malo (McGill University) for the gift of anti-IgG1 and IgG2a Abs. Special thanks to Maya Corminboeuf, Christelle Bogosta, Danica Albert, and Nadia Prud'homme for their valuable technical assistance and to Gregory Boivin for critical review of the text.

Disclosures

The authors have no financial conflict of interest.

References

1. Sinclair, J., and P. Sissons. 2006. Latency and reactivation of human cytomegalovirus. *J. Gen. Virol.* 87: 1763–1779.
2. Mocarski, E. S., Jr. 2002. Immunomodulation by cytomegaloviruses: manipulative strategies beyond evasion. *Trends Microbiol.* 10: 332–339.
3. Tay, C. H., and R. M. Welsh. 1997. Distinct organ-dependent mechanisms for the control of murine cytomegalovirus infection by natural killer cells. *J. Virol.* 71: 267–275.
4. Orange, J. S., and C. A. Biron. 1996. An absolute and restricted requirement for IL-12 in natural killer cell IFN-γ production and antiviral defense: studies of natural killer and T cell responses in contrasting viral infections. *J. Immunol.* 156: 1138–1142.
5. Biron, C. A., K. S. Byron, and J. L. Sullivan. 1989. Severe herpesvirus infections in an adolescent without natural killer cells. *N. Engl. J. Med.* 320: 1731–1735.
6. Shellam, G. R., J. E. Allan, J. M. Papadimitriou, and G. J. Bancroft. 1981. Increased susceptibility to cytomegalovirus infection in beige mutant mice. *Proc. Natl. Acad. Sci. USA* 78: 5104–5108.
7. Bukowski, J. F., B. A. Woda, S. Habu, K. Okumura, and R. M. Welsh. 1983. Natural killer cell depletion enhances virus synthesis and virus-induced hepatitis in vivo. *J. Immunol.* 131: 1531–1538.
8. Welsh, R. M., P. L. Dundon, E. E. Eynon, J. O. Brubaker, G. C. Koo, and C. L. O'Donnell. 1990. Demonstration of the antiviral role of natural killer cells in vivo with a natural killer cell-specific monoclonal antibody (NK 1.1). *Nat. Immun. Cell Growth Regul.* 9: 112–120.
9. Dalod, M., T. P. Salazar-Mather, L. Malmgaard, C. Lewis, C. Asselin-Paturel, F. Briere, G. Trinchieri, and C. A. Biron. 2002. Interferon α/β and interleukin 12 responses to viral infections: pathways regulating dendritic cell cytokine expression in vivo. *J. Exp. Med.* 195: 517–528.
10. Scalzo, A. A., N. A. Fitzgerald, A. Simmons, A. B. La Vista, and G. R. Shellam. 1990. Cmv-1, a genetic locus that controls murine cytomegalovirus replication in the spleen. *J. Exp. Med.* 171: 1469–1483.

11. Scalzo, A. A., N. A. Fitzgerald, C. R. Wallace, A. E. Gibbons, Y. C. Smart, R. C. Burton, and G. R. Shellam. 1992. The effect of the Cmv-1 resistance gene, which is linked to the natural killer cell gene complex, is mediated by natural killer cells. *J. Immunol.* 149: 581–589.
12. Brown, M. G., A. O. Dokun, J. W. Heusel, H. R. Smith, D. L. Beckman, E. A. Blattenberger, C. E. Dubbelde, L. R. Stone, A. A. Scalzo, and W. M. Yokoyama. 2001. Vital involvement of a natural killer cell activation receptor in resistance to viral infection. *Science* 292: 934–937.
13. Lee, S. H., S. Girard, D. Macina, M. Busa, A. Zafer, A. Belouchi, P. Gros, and S. M. Vidal. 2001. Susceptibility to mouse cytomegalovirus is associated with deletion of an activating natural killer cell receptor of the C-type lectin superfamily. *Nat. Genet.* 28: 42–45.
14. Daniels, K. A., G. Devora, W. C. Lai, C. L. O'Donnell, M. Bennett, and R. M. Welsh. 2001. Murine cytomegalovirus is regulated by a discrete subset of natural killer cells reactive with monoclonal antibody to Ly49H. *J. Exp. Med.* 194: 29–44.
15. Lee, S. H., A. Zafer, Y. de Repentigny, R. Kothary, M. L. Tremblay, P. Gros, P. Duplay, J. R. Webb, and S. M. Vidal. 2003. Transgenic expression of the activating natural killer receptor Ly49H confers resistance to cytomegalovirus in genetically susceptible mice. *J. Exp. Med.* 197: 515–526.
16. Scalzo, A. A., M. G. Brown, D. T. Chu, J. W. Heusel, W. M. Yokoyama, and C. A. Forbes. 1999. Development of intra-natural killer complex (NKC) recombinant and congenic mouse strains for mapping and functional analysis of NK cell regulatory loci. *Immunogenetics* 49: 238–241.
17. Sjolin, H., E. Tomasello, M. Mousavi-Jazi, A. Bartolazzi, K. Karre, E. Vivier, and C. Cerboni. 2002. Pivotal role of KARAP/DAP12 adaptor molecule in the natural killer cell-mediated resistance to murine cytomegalovirus infection. *J. Exp. Med.* 195: 825–834.
18. Arase, H., E. S. Mocarski, A. E. Campbell, A. B. Hill, and L. L. Lanier. 2002. Direct recognition of cytomegalovirus by activating and inhibitory NK cell receptors. *Science* 296: 1323–1326.
19. Smith, H. R., J. W. Heusel, I. K. Mehta, S. Kim, B. G. Dorner, O. V. Naidenko, K. Iizuka, H. Furukawa, D. L. Beckman, J. T. Pingel, et al. 2002. Recognition of a virus-encoded ligand by a natural killer cell activation receptor. *Proc. Natl. Acad. Sci. USA* 99: 8826–8831.
20. Dorner, B. G., H. R. Smith, A. R. French, S. Kim, J. Poursine-Laurent, D. L. Beckman, J. T. Pingel, R. A. Kroczek, and W. M. Yokoyama. 2004. Coordinate expression of cytokines and chemokines by NK cells during murine cytomegalovirus infection. *J. Immunol.* 172: 3119–3131.
21. Dokun, A. O., S. Kim, H. R. Smith, H. S. Kang, D. T. Chu, and W. M. Yokoyama. 2001. Specific and nonspecific NK cell activation during virus infection. *Nat. Immunol.* 2: 951–956.
22. Bubic, I., M. Wagner, A. Krmpotic, T. Saulig, S. Kim, W. M. Yokoyama, S. Jonjic, and U. H. Koszinowski. 2004. Gain of virulence caused by loss of a gene in murine cytomegalovirus. *J. Virol.* 78: 7536–7544.
23. Yokoyama, W. M., and B. F. Plougastel. 2003. Immune functions encoded by the natural killer gene complex. *Nat. Rev. Immunol.* 3: 304–316.
24. Pereira, R. A., A. Scalzo, and A. Simmons. 2001. Cutting edge: a NK complex-linked locus governs acute versus latent herpes simplex virus infection of neurons. *J. Immunol.* 166: 5869–5873.
25. Delano, M. L., and D. G. Brownstein. 1995. Innate resistance to lethal mousepox is genetically linked to the NK gene complex on chromosome 6 and correlates with early restriction of virus replication by cells with an NK phenotype. *J. Virol.* 69: 5875–5877.
26. Hansen, D. S., K. J. Evans, M. C. D'Ombrain, N. J. Bernard, A. C. Sexton, L. Buckingham, A. A. Scalzo, and L. Schofield. 2005. The natural killer complex regulates severe malarial pathogenesis and influences acquired immune responses to *Plasmodium berghei* ANKA. *Infect. Immun.* 73: 2288–2297.
27. Beebe, A. M., S. Mauze, N. J. Schork, and R. L. Coffman. 1997. Serial backcross mapping of multiple loci associated with resistance to *Leishmania major* in mice. *Immunity* 6: 551–557.
28. Hansen, D. S., M. A. Siomos, L. Buckingham, A. A. Scalzo, and L. Schofield. 2003. Regulation of murine cerebral malaria pathogenesis by CD1d-restricted NKT cells and the natural killer complex. *Immunity* 18: 391–402.
29. Parker, A. K., S. Parker, W. M. Yokoyama, J. A. Corbett, and R. M. Buller. 2007. Induction of natural killer cell responses by ectromelia virus controls infection. *J. Virol.* 81: 4070–4079.
30. Scharton, T. M., and P. Scott. 1993. Natural killer cells are a source of interferon γ that drives differentiation of $CD4^+$ T cell subsets and induces early resistance to *Leishmania major* in mice. *J. Exp. Med.* 178: 567–577.
31. Depatie, C., E. Muise, P. Lepage, P. Gros, and S. M. Vidal. 1997. High-resolution linkage map in the proximity of the host resistance locus *Cmv1*. *Genomics* 39: 154–163.
32. Zhang, W. W., and G. Matlashewski. 2004. In vivo selection for *Leishmania donovani* miniexon genes that increase virulence in *Leishmania major*. *Mol. Microbiol.* 54: 1051–1062.
33. Karupiah, G., T. N. Fredrickson, K. L. Holmes, L. H. Khairallah, and R. M. Buller. 1993. Importance of interferons in recovery from mousepox. *J. Virol.* 67: 4214–4226.
34. Adam, S. G., A. Caraux, N. Fodil-Cornu, J. C. Loredo-Osti, S. Lesjean-Pottier, J. Jaubert, I. Bubic, S. Jonjic, J. L. Guenet, S. M. Vidal, and F. Colucci. 2006. Cmv4, a new locus linked to the NK cell gene complex, controls innate resistance to cytomegalovirus in wild-derived mice. *J. Immunol.* 176: 5478–5485.
35. Salazar-Mather, T. P., J. S. Orange, and C. A. Biron. 1998. Early murine cytomegalovirus (MCMV) infection induces liver natural killer (NK) cell inflammation and protection through macrophage inflammatory protein 1α (MIP-1α)-dependent pathways. *J. Exp. Med.* 187: 1–14.
36. Biron, C. A., H. C. Su, and J. S. Orange. 1996. Function and regulation of natural killer (NK) cells during viral infections: characterization of responses in vivo. *Methods* 9: 379–393.
37. Ruzek, M. C., A. H. Miller, S. M. Opal, B. D. Pearce, and C. A. Biron. 1997. Characterization of early cytokine responses and an interleukin (IL)-6-dependent pathway of endogenous glucocorticoid induction during murine cytomegalovirus infection. *J. Exp. Med.* 185: 1185–1192.
38. Delale, T., A. Paquin, C. Asselin-Paturel, M. Dalod, G. Brizard, E. E. Bates, P. Kastner, S. Chan, S. Akira, A. Vicari, et al. 2005. MyD88-dependent and -independent murine cytomegalovirus sensing for IFN-α release and initiation of immune responses in vivo. *J. Immunol.* 175: 6723–6732.
39. Ljunggren, H. G., C. Ohlen, P. Hoglund, L. Franksson, and K. Karre. 1991. The RMA-S lymphoma mutant; consequences of a peptide loading defect on immunological recognition and graft rejection. *Int. J. Cancer* 6: 38–44.
40. Idris, A. H., H. R. Smith, L. H. Mason, J. R. Ortaldo, A. A. Scalzo, and W. M. Yokoyama. 1999. The natural killer gene complex genetic locus Chok encodes Ly-49D, a target recognition receptor that activates natural killing. *Proc. Natl. Acad. Sci. USA* 96: 6330–6335.
41. Elsner, L., V. Muppala, M. Gehrmann, J. Lozano, D. Malzahn, H. Bickeboller, E. Brunner, M. Zientkowska, T. Herrmann, L. Walter, et al. 2007. The heat shock protein HSP70 promotes mouse NK cell activity against tumors that express inducible NKG2D ligands. *J. Immunol.* 179: 5523–5533.
42. Orange, J. S., B. Wang, C. Terhorst, and C. A. Biron. 1995. Requirement for natural killer cell-produced interferon γ in defense against murine cytomegalovirus infection and enhancement of this defense pathway by interleukin 12 administration. *J. Exp. Med.* 182: 1045–1056.
43. Orange, J. S., T. P. Salazar-Mather, S. M. Opal, and C. A. Biron. 1997. Mechanisms for virus-induced liver disease: tumor necrosis factor-mediated pathology independent of natural killer and T cells during murine cytomegalovirus infection. *J. Virol.* 71: 9248–9258.
44. Bukowski, J. F., B. A. Woda, and R. M. Welsh. 1984. Pathogenesis of murine cytomegalovirus infection in natural killer cell-depleted mice. *J. Virol.* 52: 119–128.
45. Bukowski, J. F., C. A. Biron, and R. M. Welsh. 1983. Elevated natural killer cell-mediated cytotoxicity, plasma interferon, and tumor cell rejection in mice persistently infected with lymphocytic choriomeningitis virus. *J. Immunol.* 131: 991–996.
46. Benedict, C. A., C. De Trez, K. Schneider, S. Ha, G. Patterson, and C. F. 2006. Ware. Specific remodeling of splenic architecture by cytomegalovirus. *PLoS Pathog.* 2: e16.
47. Sjolin, H., S. H. Robbins, G. Bessou, A. Hidmark, E. Tomasello, M. Johansson, H. Hall, F. Charifi, G. B. Karlsson Hedestam, C. A. Biron, et al. 2006. DAP12 signaling regulates plasmacytoid dendritic cell homeostasis and down-modulates their function during viral infection. *J. Immunol.* 177: 2908–2916.
48. Sell, M. S., J. F. Bale, Jr., and R. H. Giller. 1985. T-lymphocyte subpopulations and function during murine cytomegalovirus infection. *Pediatr. Res.* 19: 583–587.
49. Bekiaris, V., O. Timoshenko, T. Z. Hou, K. Toellner, S. Shakib, F. Gaspal, F. M. McConnell, S. M. Parnell, D. Withers, C. D. Buckley, et al. 2008. $Ly49H^+$ NK cells migrate to and protect splenic white pulp stroma from murine cytomegalovirus infection. *J. Immunol.* 180: 6768–6776.
50. Lucin, P., S. Jonjic, M. Messerle, B. Polic, H. Hengel, and U. H. Koszinowski. 1994. Late phase inhibition of murine cytomegalovirus replication by synergistic action of interferon-γ and tumour necrosis factor. *J. Gen. Virol.* 75: 101–110.
51. Heise, M. T., and H. W. t. Virgin. 1995. The T-cell-independent role of γ interferon and tumor necrosis factor α in macrophage activation during murine cytomegalovirus and herpes simplex virus infections. *J. Virol.* 69: 904–909.
52. Presti, R. M., J. L. Pollock, A. J. Dal Canto, A. K. O'Guin, and H. W. t. Virgin. 1998. Interferon γ regulates acute and latent murine cytomegalovirus infection and chronic disease of the great vessels. *J. Exp. Med.* 188: 577–588.
53. Beebe, A. M., D. J. Cua, and R. L. Coffman. 1999. Genetic control of T helper subset differentiation in *Leishmania major* infection of mice. *Microbes Infect.* 1: 89–94.
54. Taylor, B. A., C. Wnek, B. S. Kotlus, N. Roemer, T. MacTaggart, and S. J. Phillips. 1999. Genotyping new BXD recombinant inbred mouse strains and comparison of BXD and consensus maps. *Mamm. Genome* 10: 335–348.
55. Long, M. 2001. Evolution of novel genes. *Curr. Opin. Genet. Dev.* 11: 673–680.
56. Henthorn, P. S., O. Smithies, and D. L. Mager. 1990. Molecular analysis of deletions in the human β-globin gene cluster: deletion junctions and locations of breakpoints. *Genomics* 6: 226–237.
57. Venturin, M., C. Gervasini, F. Orzan, A. Bentivegna, L. Corrado, P. Colapietro, A. Friso, R. Tenconi, M. Upadhyaya, L. Larizza, and P. Riva. 2004. Evidence for non-homologous end joining and non-allelic homologous recombination in atypical NF1 microdeletions. *Hum. Genet.* 115: 69–80.
58. Wilhelm, B. T., L. Gagnier, and D. L. Mager. 2002. Sequence analysis of the Ly49 cluster in C57BL/6 mice: a rapidly evolving multigene family in the immune system. *Genomics* 80: 646–661.
59. Abi-Rached, L., and P. Parham. 2005. Natural selection drives recurrent formation of activating killer cell immunoglobulin-like receptor and Ly49 from inhibitory homologues. *J. Exp. Med.* 201: 1319–1332.
60. Crozat, K., K. Hoebe, S. Ugolini, N. A. Hong, E. Janssen, S. Rutschmann, S. Mudd, S. Sovath, E. Vivier, and B. Beutler. 2007. Jinx, an MCMV susceptibility phenotype caused by disruption of Unc13d: a mouse model of type 3 familial hemophagocytic lymphohistiocytosis. *J. Exp. Med.* 204: 853–863.
61. Loh, J., D. T. Chu, A. K. O'Guin, W. M. Yokoyama, and H. W. t. Virgin. 2005. Natural killer cells utilize both perforin and γ interferon to regulate murine cytomegalovirus infection in the spleen and liver. *J. Virol.* 79: 661–667.

62. van Dommelen, S. L., N. Sumaria, R. D. Schreiber, A. A. Scalzo, M. J. Smyth, and M. A. Degli-Esposti. 2006. Perforin and granzymes have distinct roles in defensive immunity and immunopathology. *Immunity* 25: 835–848.
63. Andrews, D. M., H. E. Farrell, E. H. Densley, A. A. Scalzo, G. R. Shellam, and M. A. Degli-Esposti. 2001. NK1.1$^+$ cells and murine cytomegalovirus infection: what happens in situ? *J. Immunol.* 166: 1796–1802.
64. Gregoire, C., C. Cognet, L. Chasson, C. A. Coupet, M. Dalod, A. Reboldi, J. Marvel, F. Sallusto, E. Vivier, and T. Walzer. 2008. Intrasplenic trafficking of natural killer cells is redirected by chemokines upon inflammation. *Eur. J. Immunol.* 38: 2076–2084.
65. Salazar-Mather, T. P., and K. L. Hokeness. 2003. Calling in the troops: regulation of inflammatory cell trafficking through innate cytokine/chemokine networks. *Viral Immunol.* 16: 291–306.
66. Dalod, M., T. Hamilton, R. Salomon, T. P. Salazar-Mather, S. C. Henry, J. D. Hamilton, and C. A. Biron. 2003. Dendritic cell responses to early murine cytomegalovirus infection: subset functional specialization and differential regulation by interferon α/β. *J. Exp. Med.* 197: 885–898.
67. Robbins, S. H., G. Bessou, A. Cornillon, N. Zucchini, B. Rupp, Z. Ruzsics, T. Sacher, E. Tomasello, E. Vivier, U. H. Koszinowski, and M. Dalod. 2007. Natural killer cells promote early CD8 T cell responses against cytomegalovirus. *PLoS Pathog.* 3: e123.
68. Banks, T. A., S. Rickert, C. A. Benedict, L. Ma, M. Ko, J. Meier, W. Ha, K. Schneider, S. W. Granger, O. Turovskaya, et al. 2005. A lymphotoxin-IFN-β axis essential for lymphocyte survival revealed during cytomegalovirus infection. *J. Immunol.* 174: 7217–7225.
69. Welsh, R. M., K. Bahl, and X. Z. Wang. 2004. Apoptosis and loss of virus-specific CD8$^+$ T-cell memory. *Curr. Opin. Immunol.* 16: 271–276.
70. Carrero, J. A., B. Calderon, and E. R. Unanue. 2004. Type I interferon sensitizes lymphocytes to apoptosis and reduces resistance to *Listeria* infection. *J. Exp. Med.* 200: 535–540.
71. O'Connell, R. M., S. K. Saha, S. A. Vaidya, K. W. Bruhn, G. A. Miranda, B. Zarnegar, A. K. Perry, B. O. Nguyen, T. F. Lane, T. Taniguchi, et al. 2004. Type I interferon production enhances susceptibility to *Listeria monocytogenes* infection. *J. Exp. Med.* 200: 437–445.
72. Zucchini, N., G. Bessou, S. H. Robbins, L. Chasson, A. Raper, P. R. Crocker, and M. Dalod. 2008. Individual plasmacytoid dendritic cells are major contributors to the production of multiple innate cytokines in an organ-specific manner during viral infection. *Int. Immunol.* 20: 45–56.
73. Zucchini, N., G. Bessou, S. Traub, S. H. Robbins, S. Uematsu, S. Akira, L. Alexopoulou, and M. Dalod. 2008. Cutting edge: overlapping functions of TLR7 and TLR9 for innate defense against a herpesvirus infection. *J. Immunol.* 180: 5799–5803.
74. Krug, A., A. R. French, W. Barchet, J. A. Fischer, A. Dzionek, J. T. Pingel, M. M. Orihuela, S. Akira, W. M. Yokoyama, and M. Colonna. 2004. TLR9-dependent recognition of MCMV by IPC and DC generates coordinated cytokine responses that activate antiviral NK cell function. *Immunity* 21: 107–119.
75. Lipoldova, M., and P. Demant. 2006. Genetic susceptibility to infectious disease: lessons from mouse models of leishmaniasis. *Nat. Rev. Genet.* 7: 294–305.
76. Roberts, L. J., T. M. Baldwin, J. M. Curtis, E. Handman, and S. J. Foote. 1997. Resistance to *Leishmania major* is linked to the H2 region on chromosome 17 and to chromosome 9. *J. Exp. Med.* 185: 1705–1710.
77. Fang, M., L. L. Lanier, and L. J. Sigal. 2008. A role for NKG2D in NK cell-mediated resistance to poxvirus disease. *PLoS Pathog.* 4: e30.
78. Vercammen, E., J. Staal, and R. Beyaert. 2008. Sensing of viral infection and activation of innate immunity by Toll-like receptor 3. *Clin. Microbiol. Rev.* 21: 13–25.
79. Carrington, M., S. Wang, M. P. Martin, X. Gao, M. Schiffman, J. Cheng, R. Herrero, A. C. Rodriguez, R. Kurman, R. Mortel, et al. 2005. Hierarchy of resistance to cervical neoplasia mediated by combinations of killer immunoglobulin-like receptor and human leukocyte antigen loci. *J. Exp. Med.* 201: 1069–1075.
80. Williams, F., A. Meenagh, C. Sleator, D. Cook, M. Fernandez-Vina, A. M. Bowcock, and D. Middleton. 2005. Activating killer cell immunoglobulin-like receptor gene KIR2DS1 is associated with psoriatic arthritis. *Hum. Immunol.* 66: 836–841.
81. Martin, M. P., G. Nelson, J. H. Lee, F. Pellett, X. Gao, J. Wade, M. J. Wilson, J. Trowsdale, D. Gladman, and M. Carrington. 2002. Cutting edge: susceptibility to psoriatic arthritis: influence of activating killer Ig-like receptor genes in the absence of specific HLA-C alleles. *J. Immunol.* 169: 2818–2822.
82. Suzuki, Y., Y. Hamamoto, Y. Ogasawara, K. Ishikawa, Y. Yoshikawa, T. Sasazuki, and M. Muto. 2004. Genetic polymorphisms of killer cell immunoglobulin-like receptors are associated with susceptibility to psoriasis vulgaris. *J. Invest. Dermatol.* 122: 1133–1136.
83. Seet, B. T., and G. McFadden. 2002. Viral chemokine-binding proteins. *J. Leukocyte Biol.* 72: 24–34.
84. Reading, P. C., J. A. Symons, and G. L. Smith. 2003. A soluble chemokine-binding protein from vaccinia virus reduces virus virulence and the inflammatory response to infection. *J. Immunol.* 170: 1435–1442.
85. Smith, H. R., H. H. Chuang, L. L. Wang, M. Salcedo, J. W. Heusel, and W. M. Yokoyama. 2000. Nonstochastic coexpression of activation receptors on murine natural killer cells. *J. Exp. Med.* 191: 1341–1354.
86. Cheng, T. P., A. R. French, B. F. Plougastel, J. T. Pingel, M. M. Orihuela, M. L. Buller, and W. M. Yokoyama. 2008. Ly49h is necessary for genetic resistance to murine cytomegalovirus. *Immunogenetics* 60: 565–573.